Structural Characterization of Deployed Thermoplastic and Thermoset Composite Tidal Turbine Blades

Robynne E. Murray, Ryan Beach, Paul Murdy, Scott Dana, and Scott Hughes

National Renewable Energy Laboratory

NREL is a national laboratory of the U.S. Department of Energy
Office of Energy Efficiency & Renewable Energy
Operated by the Alliance for Sustainable Energy, LLC

This report is available at no cost from the National Renewable Energy Laboratory (NREL) at www.nrel.gov/publications.

Contract No. DE-AC36-08GO28308

Technical Report
NREL/TP-5000-88713
April 2024

Structural Characterization of Deployed Thermoplastic and Thermoset Composite Tidal Turbine Blades

Robynne E. Murray, Ryan Beach, Paul Murdy, Scott Dana, and Scott Hughes

National Renewable Energy Laboratory

Suggested Citation
Murray, Robynne E., Ryan Beach, Paul Murdy, Scott Dana, and Scott Hughes. 2024. *Structural Characterization of Deployed Thermoplastic and Thermoset Composite Tidal Turbine Blades*. Golden, CO: National Renewable Energy Laboratory. NREL/TP-5000-88713. https://www.nrel.gov/docs/fy24osti/88713.pdf.

NREL is a national laboratory of the U.S. Department of Energy
Office of Energy Efficiency & Renewable Energy
Operated by the Alliance for Sustainable Energy, LLC

This report is available at no cost from the National Renewable Energy Laboratory (NREL) at www.nrel.gov/publications.

Contract No. DE-AC36-08GO28308

Technical Report
NREL/TP-5000-88713
April 2024

National Renewable Energy Laboratory
15013 Denver West Parkway
Golden, CO 80401
303-275-3000 • www.nrel.gov

NOTICE

This work was authored by the National Renewable Energy Laboratory, operated by Alliance for Sustainable Energy, LLC, for the U.S. Department of Energy (DOE) under Contract No. DE-AC36-08GO28308. Funding provided by U.S. Department of Energy Office of Energy Efficiency and Renewable Energy Water Power Technologies Office. The views expressed herein do not necessarily represent the views of the DOE or the U.S. Government.

Cover Photos by Dennis Schroeder: (clockwise, left to right) NREL 51934, NREL 45897, NREL 42160, NREL 45891, NREL 48097, NREL 46526.

Acknowledgments

NREL thanks Verdant Power, Inc. for its significant effort in making this work possible and its ongoing dedication to progressing the tidal energy industry in the United States.

List of Acronyms

kN	kilonewton
LDT	laser distance transducer
MPa	megapascal
NREL	National Renewable Energy Laboratory
PMMA	polymethyl methacrylate
prepreg	pre-impregnated [fibers]
RRM	rated root bending moment
ue	microstrain

Executive Summary

The National Renewable Energy Laboratory (NREL) worked with Verdant Power to manufacture and characterize two-part reactive and infusible thermoplastic composite blades on the company's Gen5d 5-m diameter turbines at the Roosevelt Island Tidal Energy site in the East River in New York to demonstrate a low-cost manufacturing process for marine energy structures. Verdant had designed, manufactured, and deployed epoxy thermoset composite blades on three Gen5d turbines in October 2020. During a maintenance cycle in May 2021, a Gen5d turbine equipped with the NREL-made thermoplastic blades was deployed and retrieved in October 2021. Both the epoxy and thermoplastic blades achieved exceptional power performance during their in-water operational periods. Modal, static, and fatigue structural characterizations were performed on both blade types before and after the deployment. *This structural characterization was critical to quantifying the performance of new materials and identifying areas of concern prior to costly full scale (20+ year) turbine deployment.*

Both the epoxy and thermoplastic blades had similar static load outcomes, with the thermoplastic blades slightly stiffer than the epoxy blades. During fatigue testing, the epoxy blades performed through the 20-year accelerated life cycle. However, the blades made with the novel thermoplastic resin material failed during fatigue testing. This failure is attributed to material incompatibilities between the new thermoplastic material and existing foam and adhesive materials combined with high shear stresses in the blade at the load application location. This points to the importance of further material development to ensure that the new thermoplastic resin can be used with compatible foams, adhesives and overlay resins (which did not exist at the time of fabricating these blades). *If this issue with material incompatibilities had not been identified through this type of fatigue testing, this could have resulted in a much more costly in-water failure in the long term.* This paper provides details on thermoplastic blade manufacturing, materials, test methodology, and results.

Table of Contents

List of Figures

1 Introduction

Composite materials are typically used in marine applications due to their high strength-to-weight ratio, fatigue resistance, and resistance to harsh marine environments. Marine industries like boat building, propeller manufacturing, and tidal and river energy industries, often use fiber-reinforced thermoset composites, such as fiberglass-reinforced epoxy, for their structural components. All polymeric materials, particularly when part of a composite, exhibit some degree of degradation when subjected to marine environments due to water absorption mechanisms. When subjected to accelerated aging conditions in water at elevated temperatures, glass-reinforced epoxy composite materials can exhibit significant strength reductions when fully saturated (Davies and Arhant 2019; Davies, Le Gac, and Le Gall 2016; Nunemaker et al. 2018). Unlike conventional thermoplastics, a novel, infusible thermoplastic composite-resin systems, called Elium from Arkema Inc., has demonstrated relatively low levels of total water absorption (<0.5% total mass change) and has resistance to strength degradation due to water absorption (Davies and Arhant 2019; Davies, Le Gac, and Le Gall 2016). However, fully saturating composite laminates at elevated temperatures at the coupon scale is not necessarily representative of full-scale structures in real sea conditions for realistic operational time frames.

Furthermore, thermoset composites are also not easily recyclable at the end of life (Cousins et al. 2019). Thermoplastic composites such as Elium can be more easily recycled (Cousins et al. 2019; Cooperman, Eberle, and Lantz. 2021). Additionally, manufacturing cost estimates for wind turbine blades using a thermoplastic resin are about 5% less than costs for conventional materials (Murray et al. 2019) due to the reduced energy required for manufacturing (this thermoplastic material cures at room temperature). Due to the similarities between wind and marine energy blade structures, similar advantages of thermoplastic materials are possible for both types; however, research conducted in a real sea environment for larger-scale components is critical to understanding the value of thermoplastics to the marine industry. Therefore, NREL set out to put this new thermoplastic material to the test through an in-sea deployment and series of structural tests.

The National Renewable Energy Laboratory (NREL) worked with Verdant Power to manufacture and characterize novel thermoplastic composite blades on the company's Gen5d 5-m-diameter turbines at the Roosevelt Island Tidal Energy site in the East River in New York (see Figure 1). Epoxy blades, manufactured by a commercial subcontractor for Verdant Power, were deployed on all three turbines on Verdant's TriFrame™ in October 2020 and generated power. Six months later, the TriFrame™ was retrieved and one of the turbine rotors with epoxy blades was replaced with a turbine rotor with thermoplastic blades manufactured by NREL. The turbine rotor with thermoplastic blades was also deployed for 6 months and produced power to the New York electric grid. The details of the deployment, instrumentation, and data acquisition can be found in (Murray et al. 2023).

NREL structurally characterized both blade types before and after deployment, enabling a side-by-side comparison of the blade structures. The goal of this work was to compare the structural properties of thermoplastic-fiberglass composite blades to epoxy-fiberglass composite blades in seawater at a tidal energy site on an operational turbine, and to demonstrate a low-cost manufacturing process for marine energy structures. This development of a new material could result in a step change improvement in the cost and performance of materials used for marine energy devices. This paper outlines the materials,

manufacturing, and structural characterization of these blades before deployment (dry) and after 6 months of deployment (post-deployed).

In an ideal case, the level of blade saturation after the deployment would be quantified; however, the blades were rigidly adhered to the hub and could not be removed after deployment. Consequently, the weight differences of the rotor before and after deployment were in the noise of the measuring equipment. Therefore, we refer to the blades as "post-deployed" instead of saturated, because we do not have enough data at this time to know what level of saturation they were at after the 6-month deployments. Based on initial data from a 6 month in-water deployment, it is unlikely that the thick composite laminates being used for tidal and river energy converters will become fully saturated under realistic subsea conditions and timelines (Kennedy et al. 2018; Murdy et al. 2023). Tests are ongoing to monitor water uptake of a blade that started dry and was put in a soak tank in the laboratory to better understand water uptake. Thus far, water uptake for both blade types has been slow, but complete results are forthcoming (Murdy et al. 2023).

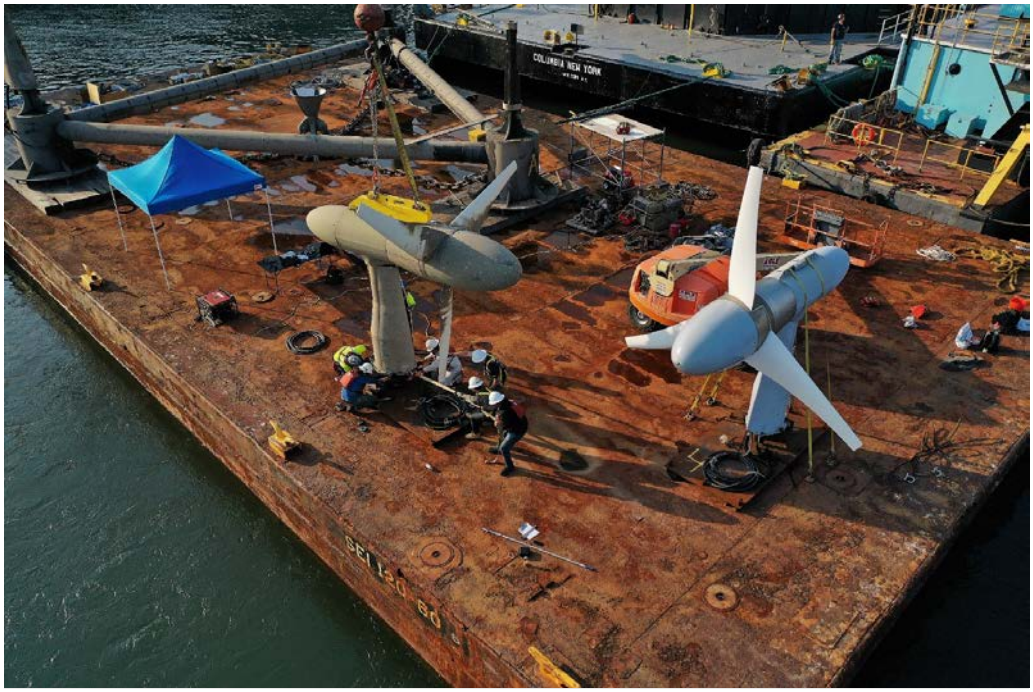

Figure 1. Verdant Power TriFrame™ and Gen5d turbines showing a turbine with epoxy blades after retrieval (left) and a turbine with thermoplastic blades (right) prior to deployment.

Photo from Paul Komosinski

2 Materials and Manufacturing

Epoxy composite blades that are 2.5 m long were manufactured by a Verdant Power subcontractor using epoxy fiberglass pre-impregnated (prepreg) fibers (rotor diameter is 5 m, but the first 0.5 m of the blade root is imbedded into the blade hub). Because the epoxy prepreg blades were already designed and manufactured prior to the start of this project, the thermoplastic blade materials were selected to match the epoxy blades according to the blade laminate schedule as closely as possible. To do this, the fiber area weights for the thermoplastic blades were matched to those of the epoxy blades, and the same layup was used for both blades with only the resin material and bonding adhesive being different. This was supported by structural modeling and mechanical testing (discussed later). A similar design and manufacturing process was used for a 13-m thermoplastic wind turbine made and validated by NREL (Murray et al. 2021); this design and process are typical in the wind industry when switching between fiberglass materials.

Thermoplastic blades with close to identical external geometry were manufactured by NREL using the same molds as for the epoxy blades, using vacuum-assisted resin transfer molding with a two-part reactive thermoplastic resin called Elium and 1,200 grams per square meter (gsm) Seartex unidirectional and 600-gsm Seartex biaxial fabrics. This fiberglass fabric is different from the epoxy blades because the epoxy blade prepreg fiberglass fabrics were not available in a dry (non-prepreg) form; instead, the area weights of the fabrics were matched. Elium is a two-part reactive acrylic-based resin made by Arkema Inc. It can be used similarly to thermoset epoxies, whereby it is mixed from two parts, infused into a fiberglass or carbon fiber fabric, and undergoes a chemical reaction to cure. Thus, it is a possible alternative for epoxy systems. This means it is feasible for use not only in a lab-scale manufacturing facility but also in typical composite manufacturing facilities. Furthermore, the vacuum-assisted resin transfer molding process is a much less expensive and energy-consuming process than prepreg and autoclave manufacturing, though generally prepreg materials have higher quality and better fatigue properties due to typically higher fiber volume fractions.

High- and low-pressure skins were infused with the two-part Elium thermoplastic resin and cured at room temperature, per the Elium manufacturer's instructions from Arkema. Internal strain gauges were applied to the blade skins, and wires were routed out through the root (see details for strain gauge methods in Murray et al. [2023]). The two skins were then bonded together with Plexus MA120 and filled with 600 kg/m^3 of Sicomin foaming epoxy (the same foam as used in the epoxy blades because a thermoplastic equivalent was not available). From previous work, we knew that polymethyl methacrylate (PMMA) adhesives adhere well to Elium thermoplastic resin (Cousins et al. 2018), whereas epoxy adhesives do not. Single-lap shear coupons made using two PMMA adhesives—Plexus and Bostik—were manufactured with 3-mm bond gaps and aged at 60°C seawater for 3 months. Both sets of specimens had average seawater uptake of about 0.7%, but the PMMA adhesives had higher static lap-shear strength both prior to and after aging; hence, PMMA was chosen to bond the thermoplastic blade skins. Lap shear testing was also performed for the epoxy foam core material to determine how well the foam adheres to the thermoplastic resin composites. The lap shear strength of the foam bonded to a thermoplastic composite specimen was significantly less than the strength of the foam bonded to an epoxy specimen (13 megapascals (MPa) lap shear strength for epoxy-epoxy bond, and 4-MPa shear strength for thermoplastic-epoxy bond). This difference suggests that the epoxy foam is not as compatible with the thermoplastic materials used here; however, at the time of this work there was not a feasible thermoplastic foam substitute, and therefore the thermoplastic blades were manufactured with the epoxy foam core. None of these materials were tested in fatigue prior to the deployment.

The final steps in the manufacturing process included a leading-edge overlay with an Arkema hand layup thermoplastic resin and final trimming and finishing. Both the epoxy and thermoplastic blades were coated using Interlux Epoxy Primekote and VC Performance Epoxy paint. This paint was tested prior to the deployment and shown to be suitable with the thermoplastic composite; however, after retrieval of the turbines it was noted that the paint failed, and there were some patches of missing paint on the thermoplastic blade.

As previously mentioned, the thermoplastic resin material is not yet available in a prepreg fabric; hence, a different manufacturing method was used for the two blade types. Prepreg materials cured in autoclaves can result in high-quality laminates because of the increased consolidation pressure and controlled fiber volume fraction. To quantify the differences between the materials and manufacturing methods used for the two blade types, composite coupons from both manufacturing processes with the fiberglass and resin materials used in the respective blades were compared under tensile loading under dry conditions. Figure 2 shows the coupons being tested and the average failure stress for both material types. These coupons had four layers of fiberglass; two layers were oriented longitudinally and two were oriented transversely (lay up of [0,90,0,90]). This layup is not traditionally used for this type of testing but was what was supplied by the epoxy blade manufacturers. These tests were performed on dry specimens following ASTM 3039 and do not account for the effects of water absorption.

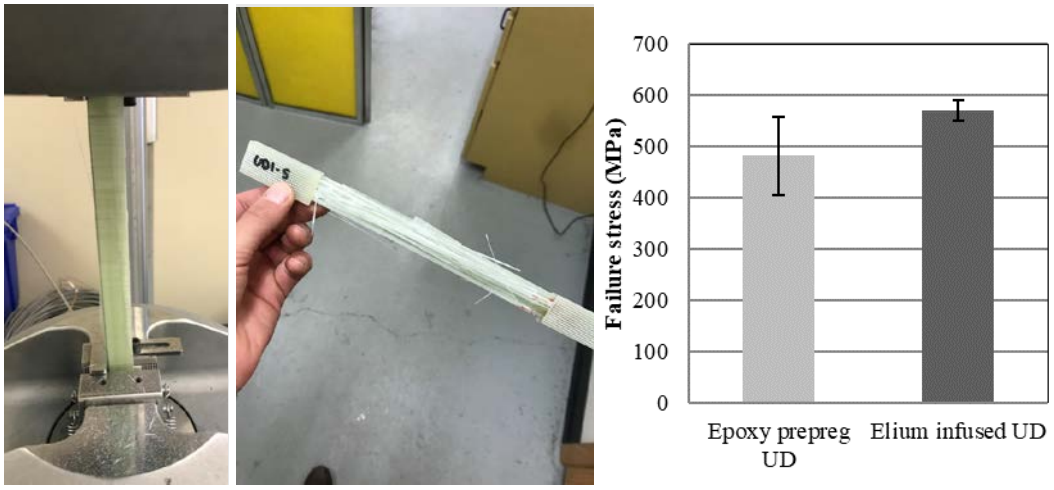

Figure 2. (Left) Coupon in load frame being tested in tension, (middle) failed coupon, (right) tensile strength of prepreg epoxy and infused thermoplastic composite coupons (dry), including error bars.

Photo by Robynne Murray, NREL

Even though the epoxy coupons were manufactured in an autoclave process and both had the same area weight of fiberglass, the infused thermoplastic coupons had 15% higher tensile strength than the epoxy coupons. Resin burn-off testing was used to quantify the coupon fiber volume fraction. It was found that the epoxy prepreg coupons had an average fiber volume fraction of 49% whereas the thermoplastic coupons had an average fiber volume fraction of 61%. This higher fiber volume fraction will typically result in higher strengths and stiffnesses. This is not typical of prepreg materials and is thought to be due to an error during epoxy blade manufacturing such as not bleeding off enough resin from the prepreg leading to higher resin content in the prepreg than is typical.

Figure 3 shows the infusion process on one of the blades and a completed high-pressure thermoplastic blade skin. Figure 4 shows a completed blade, three thermoplastic blades, and the data acquisition system on the Verdant hub ready for turbine assembly. Four blades were made in total, one for dry structural testing prior to deployment and three for deployment. Only the deployment blades were painted.

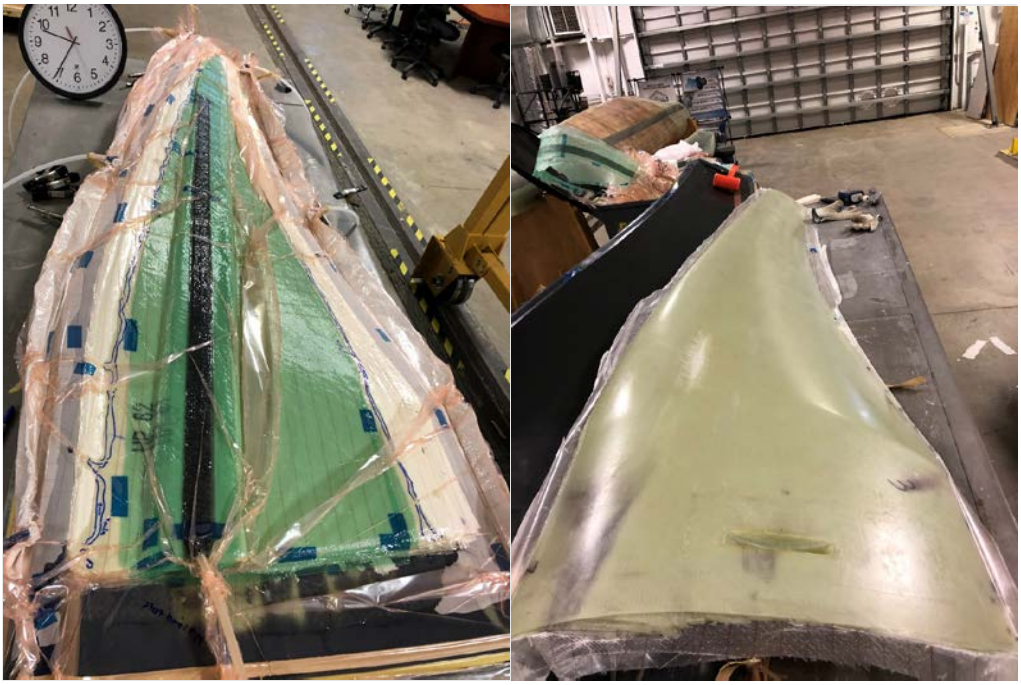

Figure 3. High-pressure thermoplastic blade skin mid-infusion (left) and completed high-pressure skin (right).

Photos by Robynne Murray, NREL

Figure 4. Completed thermoplastic blade (left) and thermoplastic blades in the Verdant Power hub ready for turbine assembly (right).

Photos by Robynne Murray, NREL

3 Test Methods

The objectives of blade structural testing were to compare the two blade types before and after deployment by measuring modal properties, deflections, and strains resulting from applied test loads. Three test methods were applied to the blades: modal property characterization, static characterization, and fatigue characterization. The post-deployed blades were bonded adhesively into a nickel-aluminum-bronze hub, as shown in Figure 4, and therefore were not able to be extracted for testing using the same setup as the pre-deployed blades. Costs prohibited the procurement of a nickel-aluminum-bronze hub to be used for pre-deployment testing of the dry blades; therefore, the pre-deployed blades were bonded into a simulated root/hub interface to connect to the test stand, whereas the post-deployed blades were tested in the full rotor configuration (see Section 3.2). This meant that the root boundary conditions for the dry and post-deployed blades were different. The implications of this are discussed further in the Results section of this report. It should be noted that the test results presented are a function of the blade design and materials specific to these blades.

3.1 Modal Property Characterization

Prior to static and fatigue loading, the modal properties of the blades were characterized using modal impact testing. Three accelerometers were located as shown in Figure 5. Multiple locations along the blade span and in multiple chordwise directions were impacted, and the resulting frequency response function traces were used to determine system frequencies, damping, and mode shapes. It should be noted that these modal tests were done in air, not in seawater that these blades were deployed in. The frequency responses and damping may be different under water, but these tests still provide a meaningful side-by-side comparison of the structural materials.

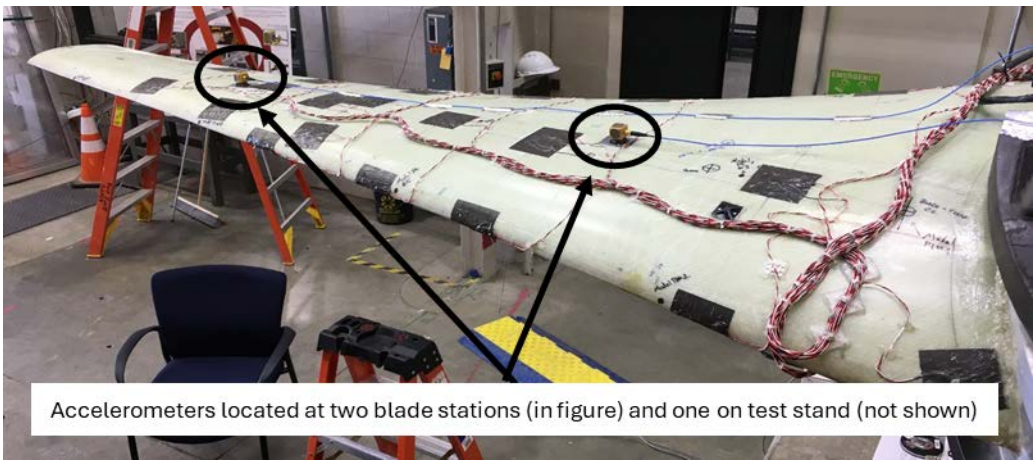

Figure 5. Thermoplastic blade on the test stand at the NREL Flatirons Campus showing set up for modal impact testing.

Photo by Scott Dana, NREL

3.2 Static and Fatigue Characterization

Only one pre-deployed blade of each material type was tested, whereas all three post-deployed blades were tested under static loading (to study manufacturing variances between blades), and one blade from each rotor (denoted Blade A) underwent the full test program outlined in the following text. Figure 6 shows the dry thermoplastic blade on the test stand and the post-deployed thermoplastic rotor with Blade A in the test stand.

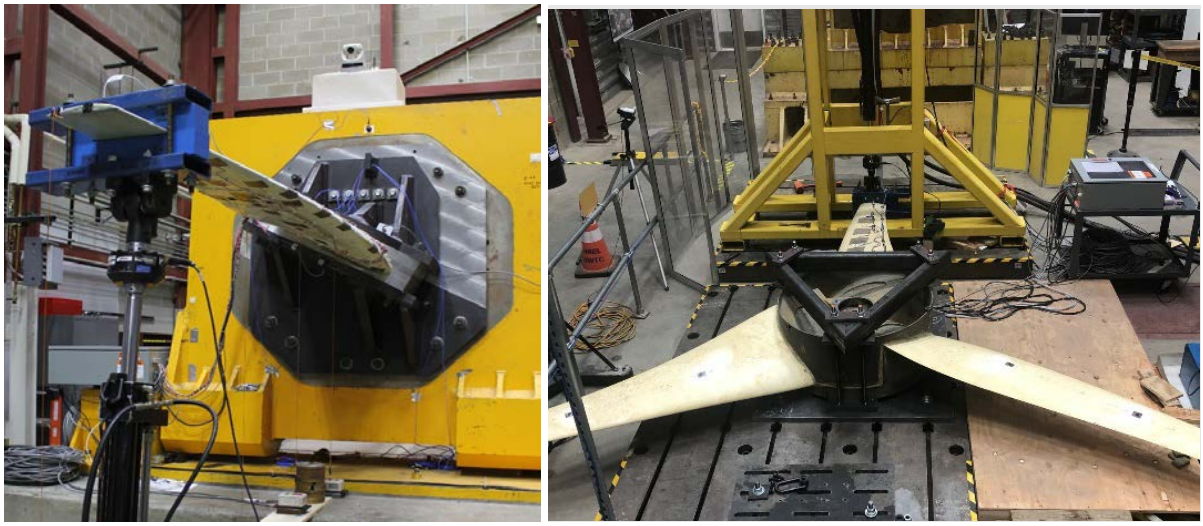

Figure 6. (Left) Dry thermoplastic blade on the test stand ready for static loading. (Right) Post-deployed thermoplastic rotor with Blade A in the test stand ready for static loading.

Photos by Ryan Beach, NREL

Test loads were applied to the blade by an MTS 247.11 single-ended hydraulic actuator with a 10,400-lb (46 kilonewtons (kN)) compression rating and 40-in. stroke. The actuator was fixed to the laboratory floor through a T-slot base plate and connected to the blade through a load introduction saddle mounted at the 2.25-m radial station (2.25 m from the center of the hub). Note that the rotor is 5 m in diameter, and the blades are 2.5 m long but embedded into the hub so that the edge of the hub and effective start of the blade is at a radial location of 0.5 m. The saddle was constructed of an outer steel frame, a wood form to match the blade profile, and rubber between the wood and the blade. A 50-kN MTS series 348910 load cell was positioned between the hydraulic actuator and the load introduction saddle and used to measure the applied test loads.

The target maximum blade root moments were provided to NREL from Verdant Power and were based on OpenFAST performance modeling. To protect Verdant Power intellectual property, the loads will be referred to as rated root bending moment (RRM), which is 50% of the maximum bending moment predicted during extreme conditions, and the rated applied force, which is the force applied by the saddle at the 2.25-m radial location to generate the RRM. Fifty percent of the maximum load was used because initial static testing showed strains over 5000 microstrain (ue) at this load level in some areas of the blade, which according to blade test standards and previous experience at NREL may lead to damage of the blade. Therefore, it was decided to not load the blade any higher than 50% of the extreme bending moment. Future testing will include a static load to failure which will better identify the ultimate load that the blades can go to before catastrophic failure. The load schedule had a combination of static and fatigue loading (fatigue testing was only performed on post-deployed blades, not dry blades). The load schedule started with commissioning static loads (10 static load pulls at the RRM), followed by fatigue testing for 2 million cycles, with static testing in the middle and at the end of the fatigue cycles (both sets having 10 static load pulls at RRM). Fatigue loads were operated at a maximum of 70% RRM which is the target fatigue loads given by Verdant Power.

The test was designed such that the actuator and saddle were perpendicular at the maximum load level, which means that there was a non-perpendicular angle between the actuator and saddle at lower loads. The actuator angle was measured throughout the tests and was

accounted for by calculating the additional induced moment that the actuator applied at the saddle location. This induced moment was at most 4% of the total moment applied to the blade and was added to the blade root moment presented in the following sections. This approach is not ideal because it could create nonlinearities in the blade response. The blade data are presented with respect to the applied loads, including these induced moments. An Ethercat Data Acquisition System, based on National Instruments Ethercat PXI technology, combined with custom NREL-developed LabVIEW-coded software was used to record data. All channels were scanned at 1,000 Hz, and time series data were recorded at both 100 Hz and 10 Hz for static and fatigue testing.

Up to forty single-axis resistance strain gauges (Vishay Micro-Measurements CEA-13-250UW-350) were installed on the blades for strain measurement. All the strain gauges had a nominal 350-Ω resistance and were connected in a three-wire configuration. External spar cap strain gauges were orientated at 0° (parallel with the spar cap) and were mounted on the center of the spar caps on both the high- and low-pressure sides of the blade at 750-mm, 1,100-mm, 1,300-mm, 1,500-mm, 1,575-mm and 1,750-mm spanwise locations. External leading-edge and trailing-edge strain gauges were positioned 50-mm in from the edge of the blade at 550-mm, 1,500-mm, 1,750-mm and 2,000-mm spanwise stations and oriented perpendicular to the local radial line, which originates at the rotor center of rotation. Internal strain gauges were applied to the deployed thermoplastic blades with details given in Murray et al. (2023) but are not included in this report. These internal gages were selected and calibrated for load measurements during deployment because externally applied gages could interfere with hydrofoil performance during turbine operation. These were only installed on the post-deployed blades. Internal gages are much closer to the neutral axis of the blade where the strains are lower and therefore external gages were chosen as a more accurate measure of strain during blade structural testing.

The hydraulic actuator contains a linear variable distance transducer that was used to measure displacement and provide feedback to the control system. This displacement was recorded for both static and fatigue testing. Additionally, four string potentiometers were used to measure displacement during static testing. The string potentiometers were placed at the r = 550-mm station, 1,000-mm station, 1,500-mm station, and the blade tip and were located at the 40% chord station as measured from the leading edge. The string potentiometers were positioned such that the strings are vertical (perpendicular to the laboratory floor) when the blade is at zero load. This positioning accounts for the weight of the blade and load introduction equipment. Each block of static load tests consisted of 10 repeated pulls. For the post-deployment tests, to measure motion of the blade root relative to the hub, a laser distance transducer (LDT) was placed at the blade root at a different location for each pull (50-mm, 100-mm, 200-mm, and 300-mm locations from the root face of the blade, and on the spar cap 40% from the leading edge, on the leading edge, and on the trailing edge).

4 Results and Discussion

4.1 Modal Characterization

The natural frequencies for Mode 1 (first flapwise bending), Mode 2 (first edgewise bending), and Mode 3 (second flapwise bending) for both blade types before and after deployment were within 5% of each other. The frequency values are not presented here to protect Verdant Power intellectual property. The percent damping for each mode are shown in Figure 7 for the dry and post-deployed epoxy and thermoplastic blades. These values are all for a single blade test of each blade type.

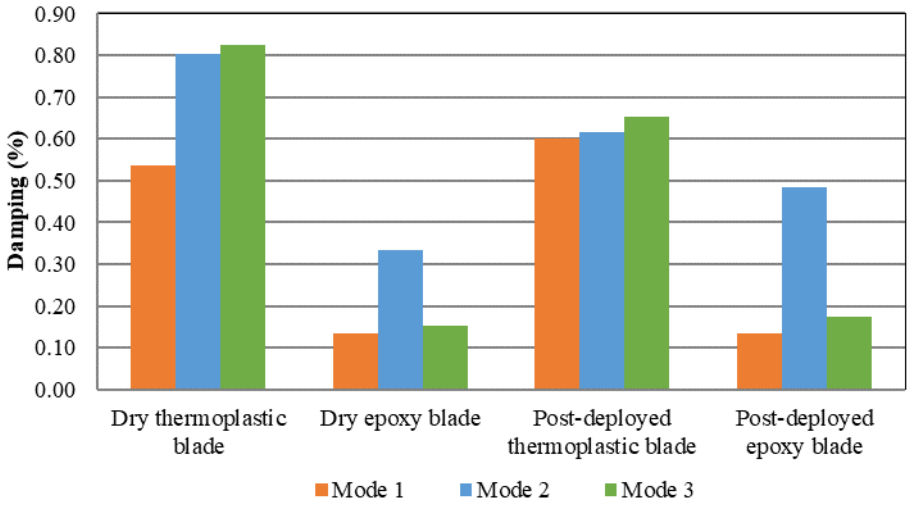

Figure 7. Modal damping properties of pre- and post-deployed thermoplastic and epoxy blades

The dry thermoplastic and epoxy blades had frequency responses within 5% of each other, with the thermoplastic blades being slightly stiffer. However, the thermoplastic blades had 3 to 4 times more damping than the epoxy blades in Mode 1 and Mode 3. The higher edgewise damping of the post-deployed epoxy blades is unexpected. These results speak to the challenges of damping estimation and the sensitivity to things like boundary conditions and the analysis method used. It was also noted that these short and relatively stiff blades had complex modes, with flapwise and edgewise modes being harder to identify separately than in large wind turbine blades. A larger sample size or repetition of experiments would help to increase accuracy of these damping values but was not possible for the one-off nature of these blades. In general, an increase in damping could have positive effects by decreasing the loads transferred to the rest of the downstream turbine components. Structural damping will be the focus of future thermoplastic blade research efforts.

4.2 Static Characterization

This section shows the results from static loading of both dry and post-deployed blades. The dry blades were loaded from below with displacement in the positive upward direction, and the post-deployed blades were loaded from above and displaced downward due to the inability to mount the entire rotor in a configuration that would enable an actuator to fit underneath it. Both are presented with the displacement in the same orientation. Blade tip displacements as a function of load are shown in Figure 8. The dry epoxy blades had more tip displacement than the thermoplastic blades, and the post-deployed epoxy blades had more tip displacement than the post-deployed thermoplastic blades. This suggests that the

thermoplastic blades are slightly stiffer which aligns with having a higher fiber volume fraction. It should be noted that because of the differences in boundary conditions there was more movement at the blade root for the post-deployed blades than for the dry blades, and hence the displacements will not be directly compared between the two test setups, as discussed in more detail in the following text.

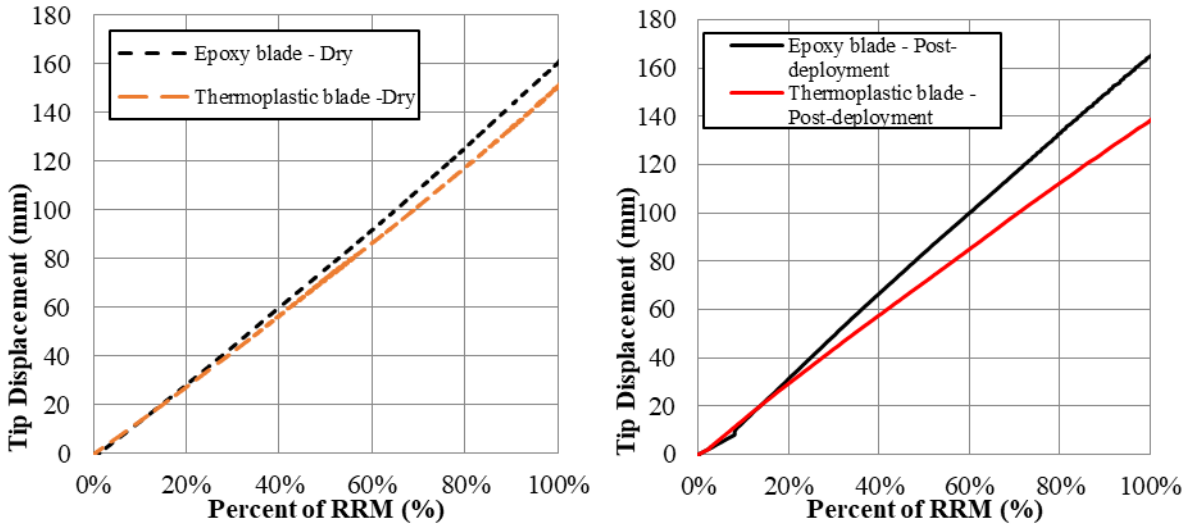

Figure 8. Epoxy and thermoplastic blade tip displacement as a function of RRM for (left) dry blades and (right) post-deployed blades

All three of the post-deployed thermoplastic blades had tip displacements within 2.85% of each other at the maximum load level, and all three of the post-deployed epoxy blades had tip displacements within 1% of each other. This suggests that manufacturing differences between the three thermoplastic blades made using vacuum infusion were relatively low, and also that the manufacturing differences between the three epoxy blades made in an autoclave process were relatively. The post-deployed epoxy blade has a nonlinearity at the 8% load level which was observed for all ten static pulls of the post-deployed epoxy blades, but not for the post-deployed thermoplastic blades. We suspect this to be a result of a setup misalignment or loose fixturing such as the saddle settling under load, however, we were not able to inspect the test setup as it was taken apart prior to data processing. Even with this nonlinearity at the start of the epoxy tests, all four blade types had highly linear displacement-load trends.

Figure 9 shows the displacements of each blade type at the RRM as measured by the LDT at various locations close to the root of the blade, and as measured by the three string potentiometers and actuator. Figure 10 shows the LDT blade root displacement measurements at locations 50 mm (root/hub interface), 100 mm, 250 mm, and 300 mm from the center of the hub. All measurements are taken at the 40% chordwise location on the spar cap of the blade.

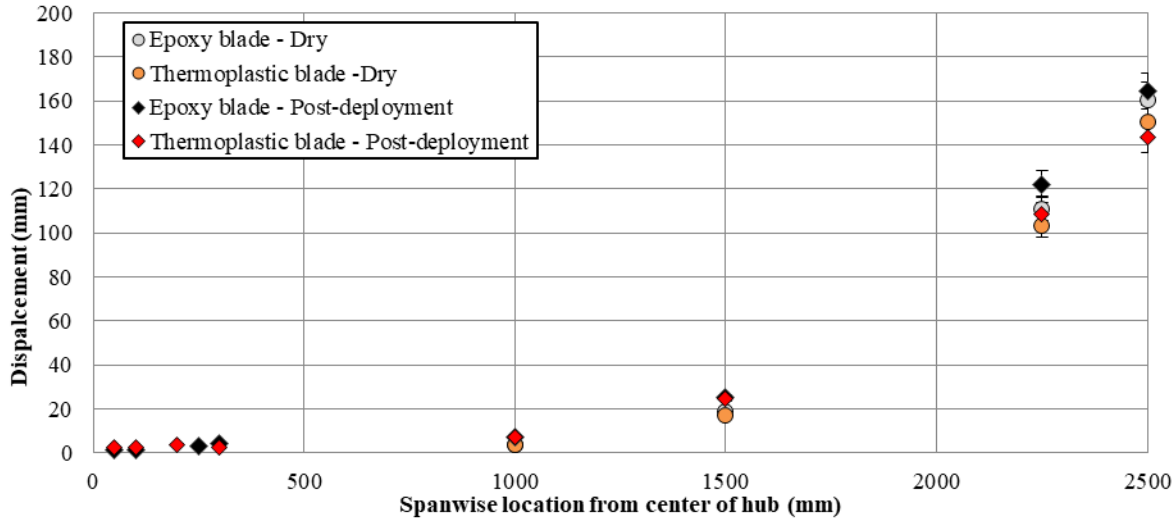

Figure 9. Spanwise displacements of epoxy and thermoplastic pre- and post-deployed blade at the RRM

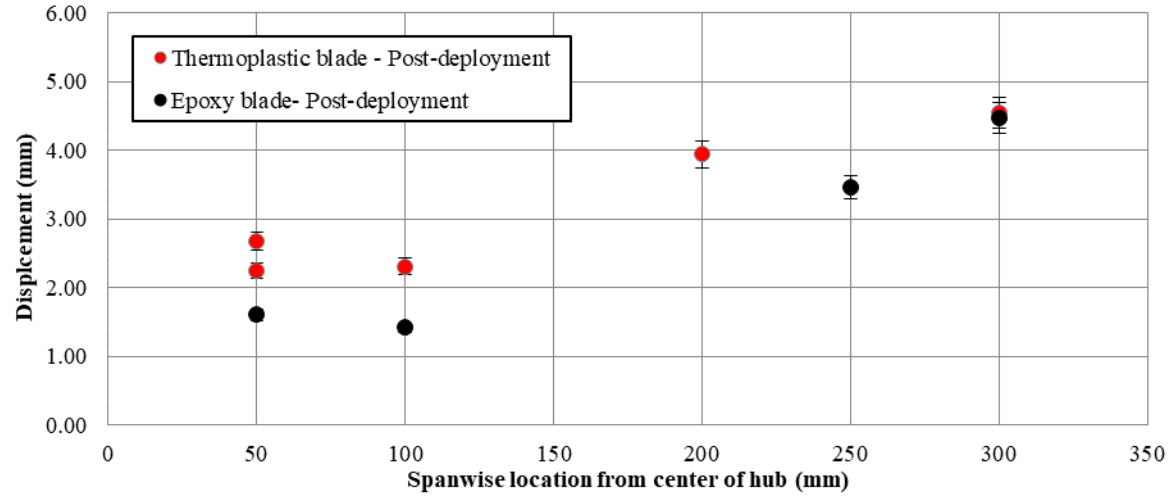

Figure 10. Spanwise displacements of epoxy and thermoplastic pre- and post-deployed blade at the RRM measured by LDT on the spar cap of blade

At 300 mm from the root of the blade, the post-deployed blades had ~4.5 mm of displacement as measured by an LDT placed at this location (shown in Figure 10), as compared to the dry blades that had less than 1 mm displacement at the root at the RRM (Figure 9). This is consistent with the less rigid boundary conditions from the test setup for the post-deployed rotor. The increased angle at the root of the post-deployed blades could, however, amplify the outboard blade displacements. For example, this increased root movement results in a blade angle of about 0.9 degrees at the root, which can have up to a 30-mm effect in the blade tip displacement for the post-deployed blades. This means that the displacements between the dry and post-deployed blades should not be directly compared. For this reason, the strain measurements make for a better side-by-side comparison for dry and post-deployed blade performance.

Figure 11 shows the tensile strains, and Figure 12 shows the compressive strains at different spanwise spar cap locations as a function of load.

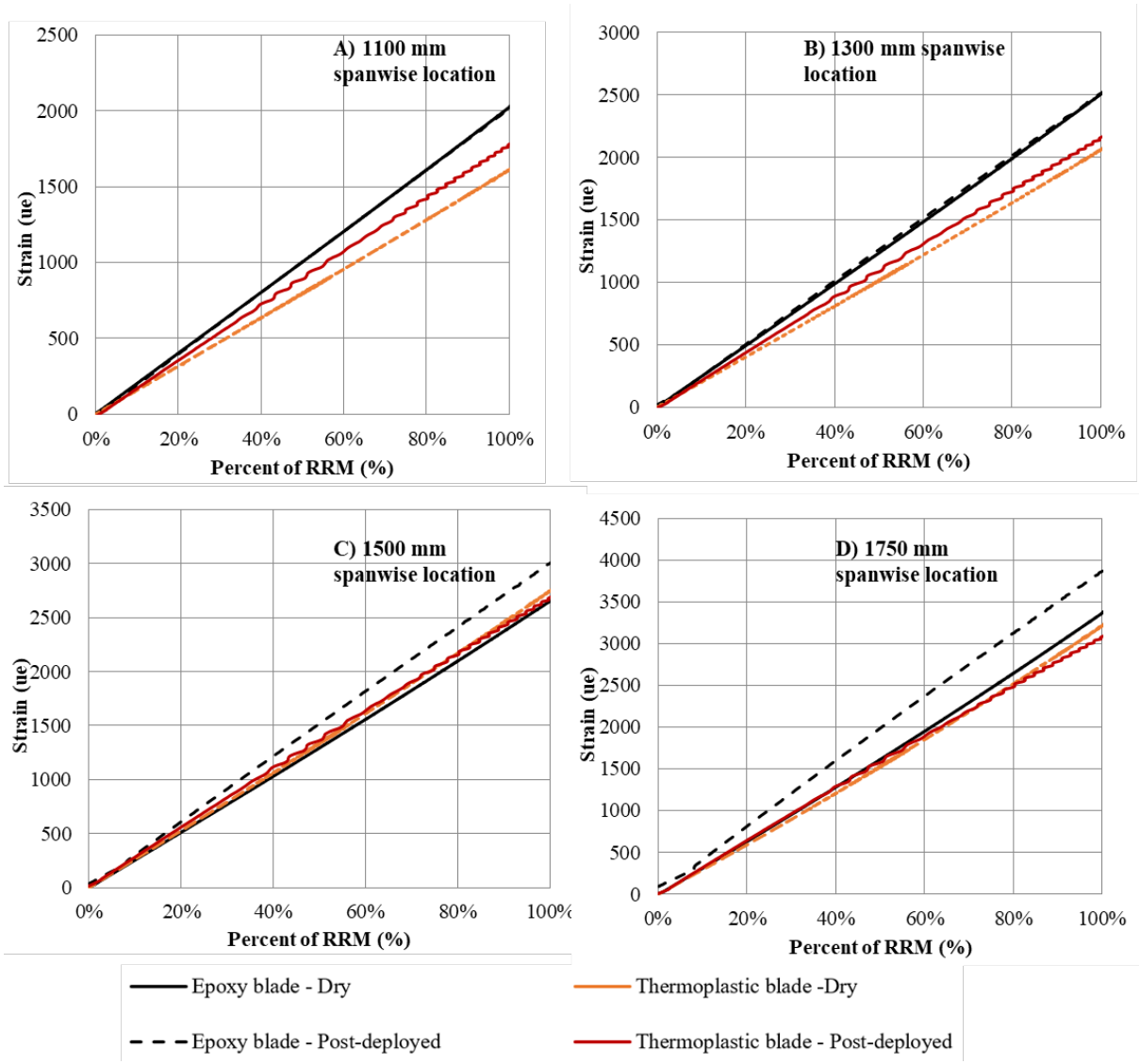

Figure 11. Epoxy and thermoplastic tensile strain at various spanwise spar cap locations as a function of applied blade root moment: (a) 1,100-mm spanwise spar cap strain gauge, (b) 1,300-mm spanwise spar cap strain gauge, (c) 1,500-mm spanwise spar cap strain gauge, (d) 1,750-mm spanwise spar cap strain gauge

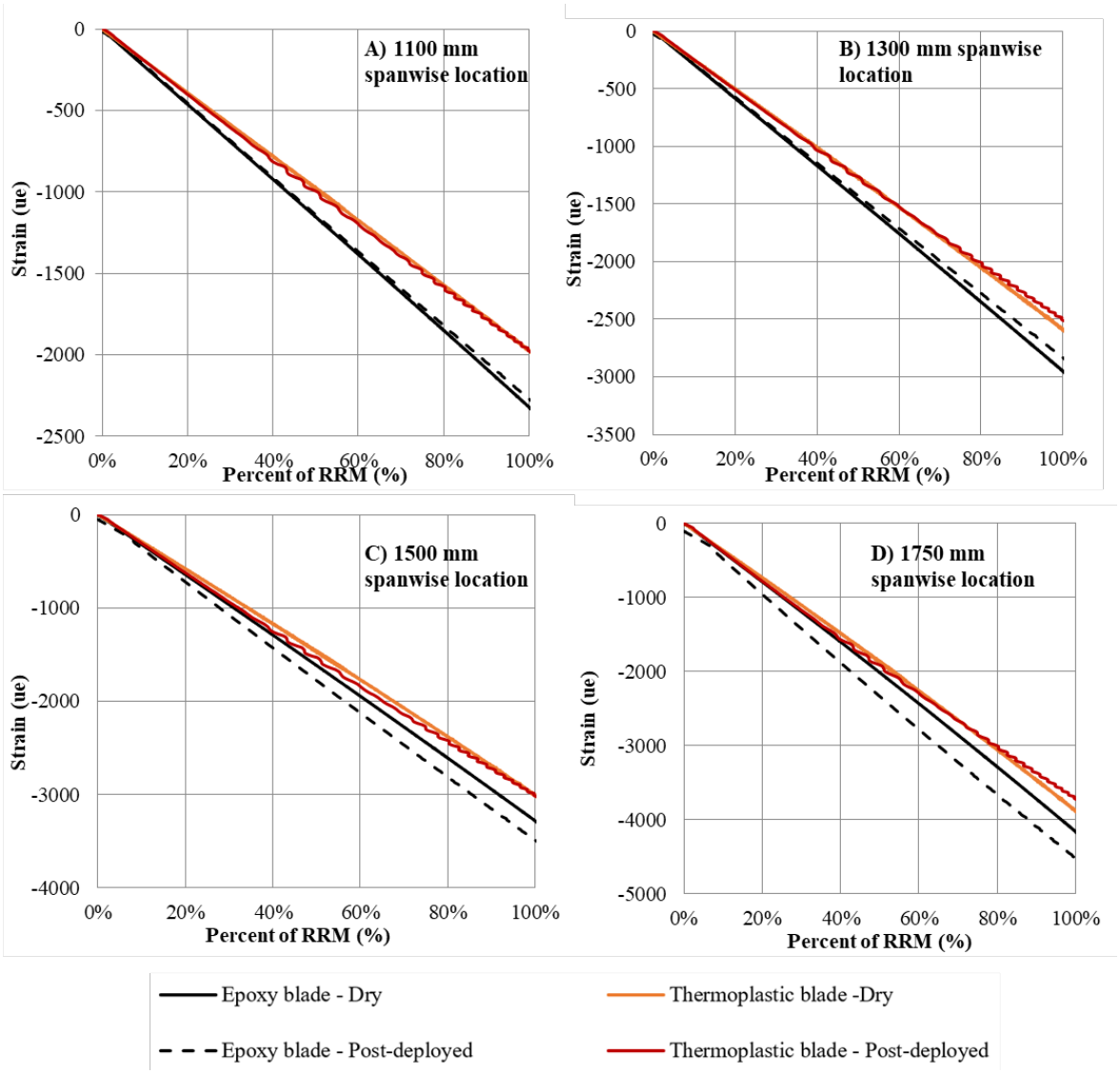

Figure 12. Epoxy and thermoplastic compressive strain at various spanwise spar cap locations as a function of applied blade root moment: (a) 1,100-mm spanwise spar cap strain gauge, (b) 1,300-mm spanwise spar cap strain gauge, (c) 1,500-mm spanwise spar cap strain gauge, (d) 1,750-mm spanwise spar cap strain gauge

Interestingly, the compressive strain in the epoxy and thermoplastic dry and post-deployed blades were very similar closer to the root of the blade (Figure 12a), but toward the outer span of the blade (Figure 12d), the post-deployed epoxy blade had an increase in strain compared to the dry blade. The compressive strain in the thermoplastic blade did not change significantly between the dry and post-deployed blades. The data also shows the post-deployed epoxy blade to have higher tensile strain toward to the tip. These differences between the dry and post-deployed epoxy blades could be due to differences in test setup, manufacturing differences, or potentially the effects of operation or seawater on the outer span of the blade where the laminate is thinner. There is uncertainty in the precise locations of the strain gauges; however, a sensitivity study using a finite element model of gauge location showed that differences of up to 3 mm would have less than 3% influence on the strain at that location.

According to Section 7.8.2.4 in the DNV-ST-0164 tidal turbine blade design standard (DNV 2021), a tensile strain of 3,500 ue and a compressive strain of 2,500 ue are generally considered conservative and may be used without material testing. These blades were

designed by a third party, and the design methodology was not disclosed; it is not clear if material testing was used to support increased strains in this blade design. The compressive strains at the test load significantly exceeded these standards, which should be considered for subsequent iterations of the blade designs.

4.3 Fatigue Characterization of Post-Deployment Blades

One of the epoxy rotor blades and two of the thermoplastic blades were loaded in fatigue after the deployment. The aim of the fatigue test was to reach 2 million cycles, simulating 20 years of operational life of the blades. For context, during the 6-month in-water operation the blades say approximately 50,000 cycles. The stiffness of the blades (Figure 13) was determined by dividing the load applied by the actuator by the displacement at the saddle location over the duration of the test. The stiffness data was smoothed to allow for easier observation of trends using a moving average filter.

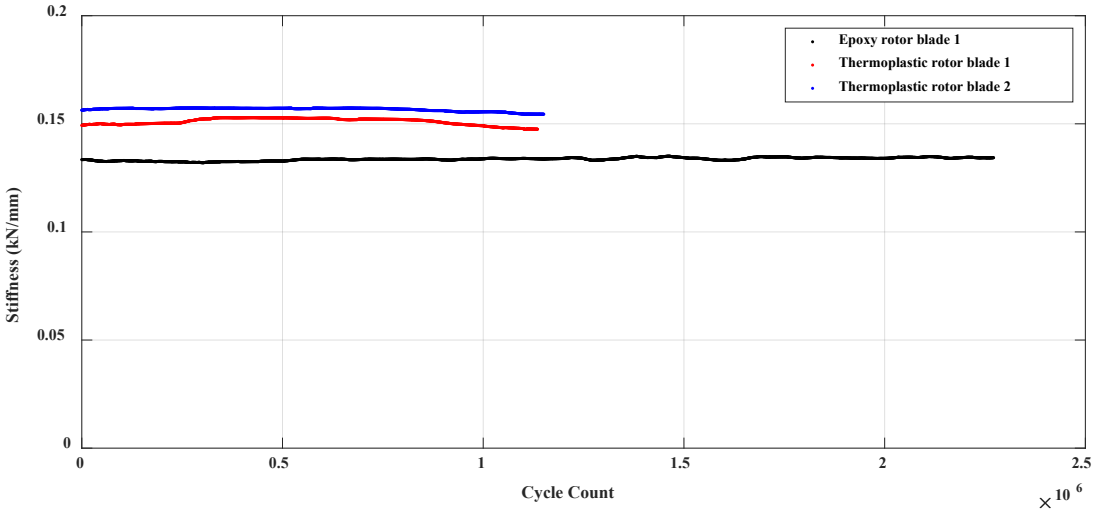

Figure 13. Blade stiffness at saddle location as a function of cycle count, smoothed data

The epoxy blades reached the full 2 million cycle test duration with no significant change in stiffness. As early as 400,000 cycles the first thermoplastic blade stiffnesses started to slowly decrease; having a 3% decrease in stiffness by 900,000 cycles. Following this, stiffnesses abruptly decreased and the test interlocks were triggered, thereby shutting down the test at 1.2 million cycles. A crack in the leading edge of the blade was observed, as shown in Figure 14, at approximately the 2,000 mm spanwise location close to the location of the saddle. The second thermoplastic blade also had a decrease in stiffness with the test operated until a small crack was observed at 1.2 million cycles. The first blade was cut from the hub and segmented spanwise to enable an internal inspection, shown in Figure 14.

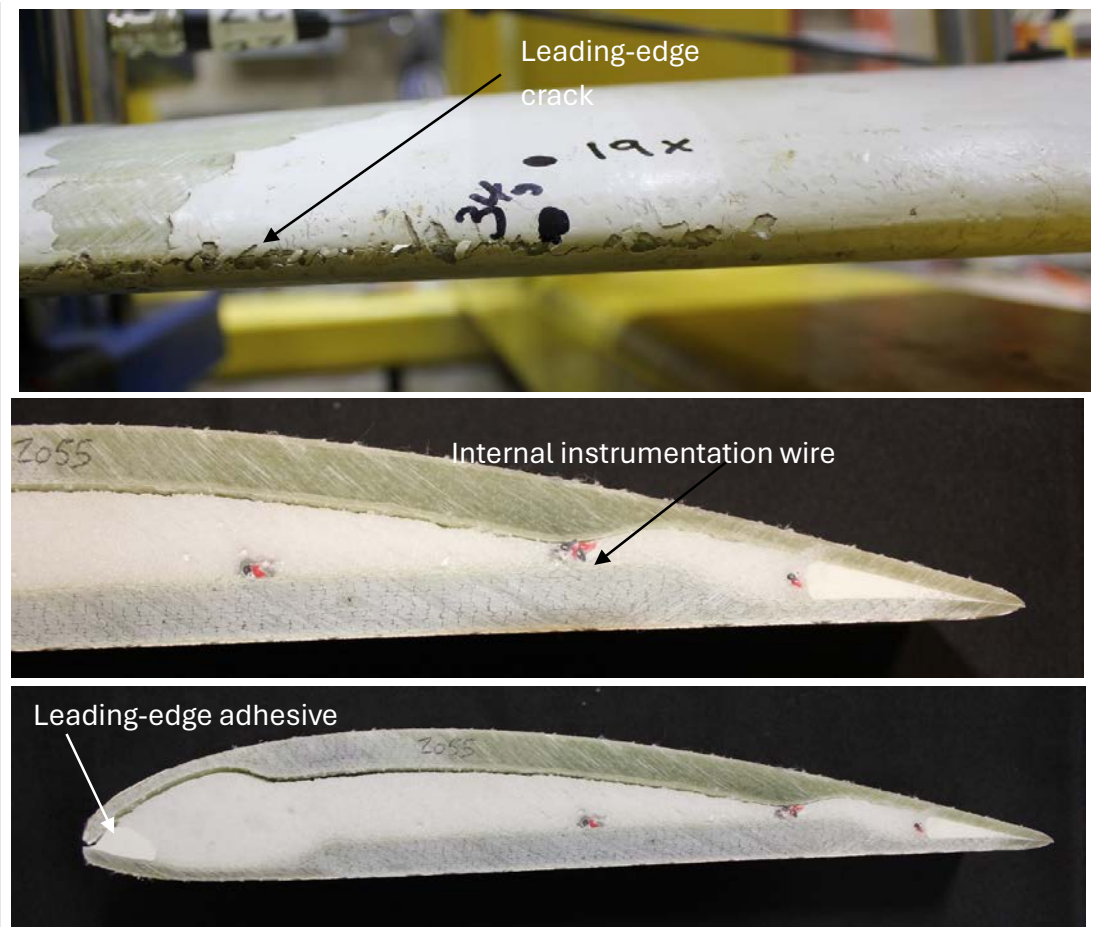

Figure 14. Leading-edge and internal damage of thermoplastic blade.

Photos by Robynne Murray, NREL

There are several potential issues that could have led to the thermoplastic blades failing in fatigue. Firstly, the application of the load at a single point on the blade led to higher shear stresses than would be realistic under real-life operational loads. Figure 15 shows the applied test loads compared to the normalized loads predicted by Verdant Power using OpenFAST for an operating turbine.

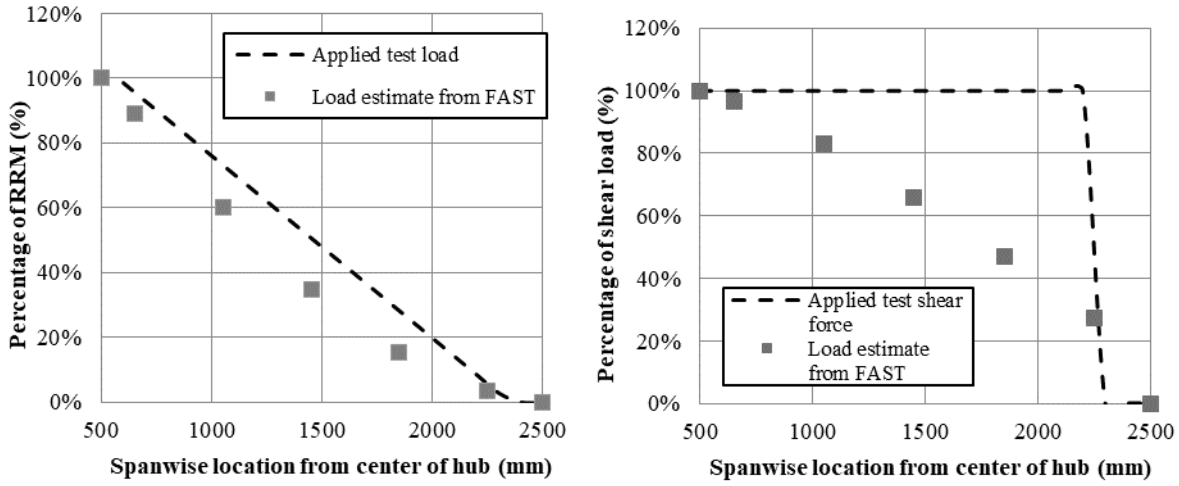

Figure 15. Applied test loads compared to predicted loads from OpenFAST model showing root bending moment and shear loads.

From Figure 15, the applied test loads track the predicted OpenFAST bending moments fairly well, however, the shear forces on the blade due to the single point applied test load are significantly higher than the shear loads that the turbine is expected to see based on OpenFAST predictions. For example, at the 2,000 mm location where the blade failure was observed, the applied shear force was 66% higher than the OpenFAST load that the blade is estimated to experience during a deployment. In a laboratory test, there are always going to be areas of a blade that are overloaded and areas that are underloaded; it's up to the blade designer to determine which areas are of most importance so that the test can be appropriately designed. In this case, limited structural design data was prohibitive to test design. For short and stiff blades such as tidal turbine blades, future tests are recommended to apply test loads at multiple points along the blade to better match the design shear loads of the blades and avoid overloading in shear.

Importantly, the foam core of these blades is critical to transferring shear loads between the two skins. As shown previously, lap shear testing between the foam and the thermoplastic suggested that the adhesion was poor due to material incompatibilities, whereas the adhesion between the epoxy laminate and the same foam core was significantly better. At the time the blades were manufactured, however, there was not a comparable thermoplastic alternative foam option. Therefore, epoxy foam was used in the thermoplastic blades. Furthermore, the leading-edge overlay on the thermoplastic blade was made using Arkema's research-grade overlay resin, which had not yet been tested for durability and was observed to not bond well to the blade. This poor adhesion of the overlay resin could also have contributed to the lack of strength in the leading edge of the blade and overstressed the adhesive bond. This problem could have been further exacerbated by the missing areas of paint coating on the thermoplastic blade leading edge, which could have caused the leading-edge overlay resin to be affected by seawater more significantly than that of the epoxy blade. These material incompatibilities will hopefully be addressed as the relatively new thermoplastic resin continues to be developed. This in-laboratory fatigue testing was critical to identifying these areas of concern with the thermoplastic materials prior to a more costly long-term in-water deployment.

Unfortunately, there were no leading-edge strain gages on the post-deployed blades (only full bridge gages were for edgewise loads which cannot be resolved into leading-edge only strains), however, multiple strain gages on the dry thermoplastic blade can be used to

estimate the leading-edge strains that the post deployed blades may have seen. From these gages, shown in Figure 16, the strains in the leading-edge of the dry thermoplastic blade were over 3,000 ue in tension and over 2,500 ue in compression at the 2,000 mm location (where the fatigue failure was observed).

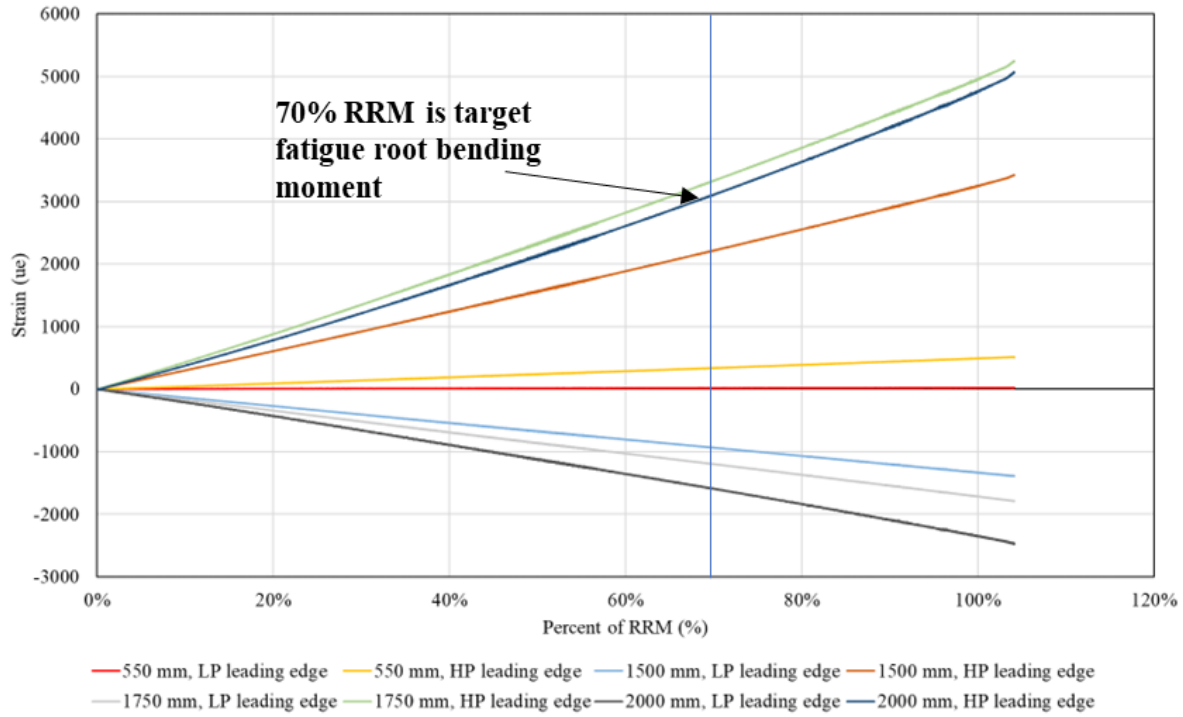

Figure 16. Dry thermoplastic blade leading edge strain gage measurements along length of blade for a static load pull. LP denotes low pressure (compression) and HP denotes high pressure (tension).

Importantly, the high strains that these blades were subjected to (over 5,000 ue at some areas of the blade) compared to what is typically recommended in blade design standards (tensile strain of 3,500 ue and a compressive strain of 2,500 ue) could have over-stressed certain areas of the blade, such as the leading edge. In general, the lack of design data and material fatigue property data makes this failure hard to fully understand.

5 Conclusions

Verdant Power designed epoxy blades that were manufactured and deployed on three Verdant Power Gen5d 5-m turbines in New York's East River in October 2020. During a maintenance cycle in May 2021, thermoplastic blades manufactured by NREL were deployed on a Gen5d turbine and removed in October 2021. Modal, static, and fatigue structural characterization were performed on both blade types before and after the deployment. *This structural characterization is critical to understanding how new materials perform and to identify areas of concern prior to full scale (20+ year) turbine deployment.* In this case, both the epoxy and thermoplastic blades had similar static load outcomes, with the thermoplastic blades slightly stiffer than the epoxy blades. During fatigue testing, the epoxy blades had no change in stiffness over the 20-year accelerated life cycle. However, the blades made with the novel thermoplastic resin failed during fatigue testing. This failure is attributed to potential material incompatibilities combined with high shear stresses in the blade at the load application location.

Even though the thermoplastic blades survived the 6-month deployment with no change in stiffness, the failure observed during fatigue testing points to the importance of further material development to ensure that the new thermoplastic resin can be used with compatible foams, paints and overlay resins (which do not yet exist). If this issue with material incompatibilities had not been identified through this type of fatigue testing, this could have resulted in a much more costly in-water failure in the long term. Even with this issue, thermoplastic resins may provide promise for future lower-cost, recyclable solutions for tidal turbine blades. With further development of thermoplastic materials, more compatible paints, foams, and fiber sizings will be developed, which will enable continued improvement in thermoplastic performance.

To further understand the effects of seawater ingress on various composite materials, one post-deployed thermoplastic blade and one epoxy blade are being conditioned in a water tank with frequent weight measurements to determine how long it takes to fully saturate each blade type. This will provide a better understanding of the blades' likely level of saturation after the 6-month deployment in the East River. In addition, composite coupon specimens were cut from one post-deployed thermoplastic blade and one epoxy blade, with half to be tested dry (the blades have now been out of water for over a year and are presumed to be fully dried) and the other half to be conditioned in seawater and tested after they reach complete saturation. This test will provide a better understanding of the effects of seawater on a large-scale composite tidal turbine blade. This work not only provides a better understanding of deployed composite materials at scale but also highlights some of the challenges of instrumenting and testing tidal turbine blades.

References

Cooperman, A., A. Eberle, and E. Lantz. 2021. "Wind Turbine Blade Material in the United States: Quantities, Costs, and End-of-Life Options." *Resources, Conservation and Recycling* 168: 105439. https://doi.org/10.1016/j.resconrec.2021.105439.

Cousins, D. S., Y. Suzuki, R. E. Murray, J. R. Samaniuk, and A. P. Stebner. 2019. "Recycling Glass Fiber Thermoplastic Composites From Wind Turbine Blades." *Journal of Cleaner Production* 209: 1252–1263. https://doi.org/10.1016/j.jclepro.2018.10.286.

Cousins, D., A. Stebner., D. Penumadu, S. Young, D. Snowberg. 2018. *Elium and Epoxy Composite Structural Comparison* in *IACMI 4.2 DOE Project Deliverable.*

Davies, P., and M. Arhant. 2019. "Fatigue Behaviour of Acrylic Matrix Composites: Influence of Seawater." *Applied Composite Materials* 26: 507–518. https://doi.org/10.1007/s10443-018-9713-1.

Davies, P., P.-Y. Le Gac, and M. Le Gall. 2017. "Influence of Sea Water Aging on the Mechanical Behaviour of Acrylic Matrix Composites." *Applied Composite Materials* 24: 97–111. https://doi.org/10.1007/s10443-016-9516-1.

DNV. 2021. Standard: DNV-ST-0164 Tidal Turbines. https://www.dnv.com/energy/standards-guidelines/dnv-st-0164-tidal-turbines.html.

Kennedy, C. R., V. Jaksic, S. B. Leen, and C. M. O. Bradáigh. 2018. "Fatigue Life of Pitch- and Stall-Regulated Composite Tidal Turbine Blades." *Renewable Energy* 121: 688–699. https://doi.org/10.1016/j.renene.2018.01.085.

Murdy, P., S. Hughes, D. Miller, F. Presuel-Moreno, G. Bonheyo, B. Hernandez-Sanchez, and B. Gunawan. 2023. "Subcomponent Validation of Composite Joints for the Marine Energy Advanced Materials Project." Golden, CO: National Renewable Energy Laboratory. NREL/TP-5700-84487. https://www.nrel.gov/docs/fy23osti/84487.pdf.

Murdy, P., R. Murray, A. Lusty, S. Hughes, R. Beach. 2024. "Post-Deployment Characterization of Glass Fiber Reinforced Thermoset and Thermoplastic Composite Tidal Turbine Blades" Long Beach ,Ca. SAMPE North America 2024 Conference Proceedings.

Murray, R. E., R. Beach, D. Barnes, D. Snowberg, D. Berry, S. Rooney, M. Jenks, et al. 2021. "Structural Validation of a Thermoplastic Composite Wind Turbine Blade With Comparison to a Thermoset Composite Blade." *Renewable Energy*164: 1100–1107. https://doi.org/10.1016/j.renene.2020.10.040.

Murray, R. E., S. Jenne, D. Snowberg, D. Berry, and D. Cousins. 2019. "Techno-Economic Analysis of a Megawatt-Scale Thermoplastic Resin Wind Turbine Blade." *Renewable Energy* 131: 111–119. https://doi.org/10.1016/j.renene.2018.07.032.

Murray, R. E., A. Simms, A. Bharath, R. Beach, M. Murphy, L. Kilcher, and A. Scholbrock. 2023. "Toward the Instrumentation and Data Acquisition of a Tidal Turbine in Real Site Conditions." *Energies* 16(3): 1255. https://doi.org/10.3390/en16031255.

Nunemaker, J. D., M. M. Voth, D. A. Miller, D. D. Samborsky, P. Murdy, and D. S. Cairns. 2018. “Effects of Moisture Absorption on Damage Progression and Strength of Unidirectional and Cross-Ply Fiberglass-Epoxy Composites.” *Wind Energy Science* 3(1): 427–438. https://doi.org/10.5194/wes-3-427-2018.